
Interpolating between sampling and variational inference with infinite stochastic mixtures

Richard D. Lange

University of Pennsylvania
lange.richard.d@gmail.com

Ari Benjamin

University of Pennsylvania

Ralf M. Haefner*

University of Rochester

Xaq Pitkow*

Baylor College of Medicine
Rice University
xaq@rice.edu

*equal contribution

Abstract

Sampling and Variational Inference (VI) are two large families of methods for approximate inference with complementary strengths. Sampling methods excel at approximating arbitrary probability distributions, but can be inefficient. VI methods are efficient, but can fail when probability distributions are complex. Here, we develop a framework for constructing intermediate algorithms that balance the strengths of both sampling and VI. Both approximate a probability distribution using a mixture of simple component distributions: in sampling, each component is a delta-function and is chosen stochastically, while in standard VI a single component is chosen to minimize divergence. We show that sampling and VI emerge as special cases of an optimization problem over a mixing distribution, and intermediate approximations arise by varying a single parameter. We then derive closed-form sampling dynamics over variational parameters that stochastically build a mixture. Finally, we discuss how to select the optimal compromise between sampling and VI given a computational budget. This work is a first step towards a highly flexible yet simple family of inference methods that combines the complementary strengths of sampling and VI.

latent variables and the likelihood function connecting them to data are known, but computing the posterior exactly is intractable. There are two largely separate families of techniques for approximating such intractable inference problems: Markov Chain Monte Carlo (MCMC) sampling, and Variational Inference (VI) (Bishop, 2006; Murphy, 2012).

Sampling-based methods, including MCMC, approximate a distribution with a finite set of representative points. MCMC methods are stochastic and sequential, generating a sequence of sample points that, given enough time, become representative of the underlying distribution increasingly well. That is, MCMC sampling is (typically) asymptotically unbiased and relatively cheap to compute per sample, at the expense of high variance, leading to potentially long run times in practice. Similar to the approach we take here, sampling methods are studied at different scales: both in terms of their asymptotic limit (i.e. their bias at infinitely many samples) and their practical behavior for finite samples or other resource limits (i.e. their variance) (Korattikara et al., 2014; Angelino et al., 2016).

Variational Inference (VI) refers to methods that produce an approximate distribution by minimizing some quantification of divergence between the approximation and the desired posterior distribution (Zhang et al., 2019). For the purposes of this paper, we will use VI to refer to the most common flavor of variational methods, namely minimizing the Kullback-Leibler (KL) divergence between an approximate distribution from a fixed family and the desired distribution (Bishop, 2006; Wainwright and Jordan, 2008; Murphy, 2012). Whereas sampling methods can be thought of as taking place “in the space of random variables,” VI takes place “in the space of parameters.” For instance, samples of a real-valued scalar are themselves real-valued scalars, but the variational problem of finding the best-fitting Gaussian is an opti-

1 INTRODUCTION

We are concerned with the familiar and general case of approximating a probability distribution, such as occurs in Bayesian inference when both the prior over

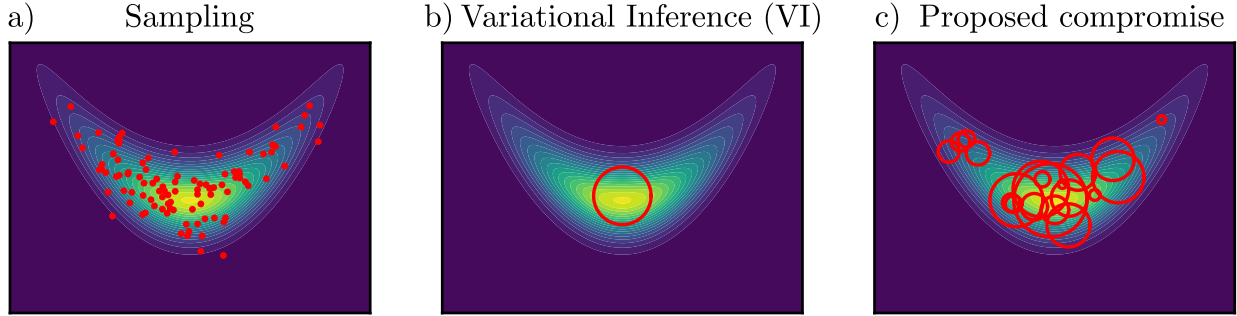


Figure 1: Conceptual introduction on a toy 2D example. **a)** Sampling methods approximate the underlying $p(\mathbf{x})$ with a stochastic set of representative points. **b)** Variational Inference (VI) methods begin by selecting an approximating distribution family, $q(\mathbf{x}; \theta)$, here an isotropic Gaussian plotted as an ellipse at its 1σ contour. The optimal parameters θ^* are chosen to minimize $\text{KL}(q(\mathbf{x}; \theta) || p(\mathbf{x}))$. **c)** We propose using a stochastic mixture of component distributions, where *parameters* θ are sampled rather than the variable of interest \mathbf{x} .

mization problem in the two-dimensional space of the Gaussian’s parameters (e.g. mean and variance). The best-fitting approximate distribution is often used directly as a proxy for the true posterior in subsequent calculations, which can greatly simplify those downstream calculations if the approximate distribution is itself easy to integrate. In contrast to MCMC, VI is often used in cases where speed is more important than asymptotic bias (Angelino et al., 2016; Zhang et al., 2019).

In this work, our goal is to develop an intermediate family of methods that “interpolate” MCMC and VI, inspired by a simple and intuitive picture (Figure 1): we propose constructing a stochastic process *in the space of variational parameters* such that the resulting approximation is a stochastic mixture of variational “component” distributions. This extends sampling by replacing the sampled points with extended components, analogous to kernel density estimation but in the space of inferred rather than observed variables. It extends VI by replacing the single best-fitting variational distribution with a stochastic mixture of more localized components. This is qualitatively distinct from previous variational methods that use *stochastic optimization*: rather than stochastically optimizing a single variational approximation (Hoffman et al., 2013; Salimans et al., 2015), we use stochasticity to construct a *random mixture* of variational components that achieves lower asymptotic bias than any one component could. We will further show below how classic sampling and classic variational inference emerge as special cases of a single optimization problem.

This paper is organized as follows. In section 2, we set up the problem and our notation, and describe how both classic sampling and classic VI can be under-

stood as mixtures. In section 3, we introduce an intuitive framework for reasoning about infinite stochastic mixture distributions, define an optimization problem over these mixtures, and state our main theoretical results in two theorems. Section 4 introduces a tractable approximation to this optimization problem from which simple closed-form sampling dynamics are derived. Section 5 discusses resource-limitations and suggests a method to find the optimal compromise between sampling and VI. Section 6 concludes with a summary, related work, limitations, and proposed future directions.

2 SETUP AND NOTATION

Let $p^*(\mathbf{x}) = Zp(\mathbf{x})$ denote the unnormalized probability distribution of interest, with unknown normalizing constant Z . For instance, in the common case of a probabilistic model with latent variables \mathbf{x} , observed data \mathcal{D} , and joint distribution $p(\mathbf{x}, \mathcal{D})$, we are interested in approximations to the posterior distribution $p(\mathbf{x}|\mathcal{D})$. This is intractable in general, but we assume that we have access to the un-normalized posterior $p^*(\mathbf{x}|\mathcal{D}) = \frac{1}{Z}p(\mathcal{D}|\mathbf{x})p(\mathbf{x})$.¹ Let $q(\mathbf{x}; \theta)$ be any “simple” distribution that may be used in a classic VI context (such as mean-field or Gaussian), and let $m_T(\mathbf{x})$ be a mixture containing T of these simple distributions as components, defined by a set of T variational (component) parameters $\{\theta^{(1)}, \dots, \theta^{(T)}\}$:

$$m_T(\mathbf{x}) \equiv \frac{1}{T} \sum_{t=1}^T q(\mathbf{x}; \theta^{(t)}). \quad (1)$$

¹To reduce clutter, \mathcal{D} will be dropped in the remainder of the paper, and we will use only $p(\mathbf{x})$ and $p^*(\mathbf{x})$.

For example, if q is a multivariate normal with mean μ and covariance Σ , then $\theta^{(t)} = \{\mu^{(t)}, \Sigma^{(t)}\}$ and $m_T(\mathbf{x})$ would be a mixture of T component normal distributions (Gershman et al., 2012).

We will study properties of distributions over component parameters, which we denote $\psi(\theta)$. If the set of $\theta^{(t)}$ is drawn randomly from $\psi(\theta)$, then as $T \rightarrow \infty$, $m_T(\mathbf{x})$ approaches the idealized infinite mixture, which we write as

$$m(\mathbf{x}) \equiv \int_{\theta} q(\mathbf{x}; \theta) \psi(\theta) d\theta. \quad (2)$$

Sampling and VI as special cases of the mixing distribution. Let $\theta^* = \arg \min_{\theta} \text{KL}(q(\mathbf{x}; \theta) \| p(\mathbf{x}))$ be the parameters corresponding to the classic single-component variational solution. VI corresponds to the special case where the mixing distribution $\psi(\theta)$ is a Dirac delta around θ^* , or $\psi(\theta) = \delta(\theta - \theta^*)$, in which case the mixture $m_T(\mathbf{x})$ is equivalent to $q(\mathbf{x}; \theta^*)$ regardless of the number of components T . Sampling can also be seen as a special case of $\psi(\theta)$ in which each component narrows to a Dirac delta (the marginal distribution of component variances concentrates around zero), and the means of the components are distributed according to $p(\mathbf{x})$. This requires that the component family $q(\mathbf{x}; \theta)$ is capable of expressing a Dirac-delta at any point \mathbf{x} . Thus, both sampling and VI can be seen as limiting cases of stochastic mixture distributions, $m_T(\mathbf{x})$, defined by a distribution over component parameters, $\psi(\theta)$. In what follows, we will show how designing the mixing distribution $\psi(\theta)$ – or indirectly constructing it by a stochastic process over θ – allows us to create mixtures that trade-off the complementary strengths of sampling and VI. Note that we will analytically study $m(\mathbf{x})$, but in practice T will be finite (discussed further in section 5).

3 OPTIMIZATION FRAMEWORK OVER MIXING DISTRIBUTIONS

3.1 Decomposing $\text{KL}(m \| p)$ Into Mutual Information and Expected KL

The idealized infinite mixture $m(\mathbf{x})$ is fully defined by the chosen component family $q(\mathbf{x}; \theta)$ and the mixing distribution $\psi(\theta)$. To construct the mixing distribution, we start by considering the variational objective with respect to the entire mixture, $\text{KL}(m \| p)$:

$$\text{KL}(m \| p) = \int_{\mathbf{x}} m(\mathbf{x}) \log \frac{m(\mathbf{x})}{p^*(\mathbf{x})} d\mathbf{x} + \log Z, \quad (3)$$

where Z is the normalizing constant of $p^*(\mathbf{x})$ and is irrelevant for constructing $m(\mathbf{x})$. Directly minimizing (3) for mixtures is intractable in general. However, as

first shown by Jaakkola and Jordan (1998) for finite mixtures, it admits the following useful decomposition:

$$\begin{aligned} \text{KL}(m \| p) &= \underbrace{\int_{\theta} \psi(\theta) \int_{\mathbf{x}} q(\mathbf{x}; \theta) \log \frac{q(\mathbf{x}; \theta)}{p^*(\mathbf{x})} d\mathbf{x} d\theta}_{\text{(i) Expected KL}} \\ &\quad - \underbrace{\int_{\theta} \psi(\theta) \int_{\mathbf{x}} q(\mathbf{x}; \theta) \log \frac{q(\mathbf{x}; \theta)}{m(\mathbf{x})} d\mathbf{x} d\theta}_{\text{(ii) Mutual Information } \mathcal{I}[\mathbf{x}; \theta]} \end{aligned} \quad (4)$$

(dropping $\log Z$). The first term, (i), is the **Expected KL Divergence** for each component when the parameters are drawn from $\psi(\theta)$. This term quantifies, on average, how well the mixture components match the target distribution. In isolation, the Expected KL is minimized when all components individually minimize $\text{KL}(q \| p)$, i.e. when $\psi(\theta) \rightarrow \delta(\theta - \theta^*)$. This tendency to concentrate $\psi(\theta)$ to the single best variational solution is balanced by the second term, (ii), which is the **Mutual Information** between \mathbf{x} and θ , which we will write $\mathcal{I}[\mathbf{x}; \theta]$, under the joint distribution $q(\mathbf{x}; \theta)\psi(\theta)$. This term should be *maximized*, and, importantly, it does not depend on $p^*(\mathbf{x})$. Mutual Information is maximized when the components are as distinct as possible, as in when the components shrink towards Dirac-delta distributions. Maximizing Mutual Information encourages the components to become narrow and to spread out over diverse regions of \mathbf{x} *regardless* of how well they agree with $p(\mathbf{x})$. This decomposition of $\text{KL}(m \| p)$ into Mutual Information (between \mathbf{x} and θ) and Expected KL (between q and p) is convenient because approximations to Mutual Information are well-studied, and minimizing Expected KL can leverage standard tools from VI.

3.2 Optimizing an Imbalanced Objective That Over-Weights Expected KL

Figure 2 depicts a two-dimensional space with Expected KL on the x-axis and Mutual Information on the y-axis. Any given mixing distribution ψ can be placed as a point in this space, but in general many ψ 's may map to the same point. We propose to view the two terms in (4) as separate objectives that may be differently weighted, i.e. maximizing the objective

$$\mathcal{L}(\psi, \lambda) = \mathcal{I}[\mathbf{x}; \theta] - \lambda \mathbb{E}_{\psi} [\text{KL}(q \| p)] \quad (5)$$

for a given hyperparameter λ with respect to the mixing distribution ψ . This objective may alternatively be viewed as a *constrained optimization* problem over the mixing density ψ , where Mutual Information is maximized subject to a constraint on Expected KL. This is a concave maximization problem with linear constraints, which implies that there is a unique optimal ψ for each λ , defining a Pareto front of solutions

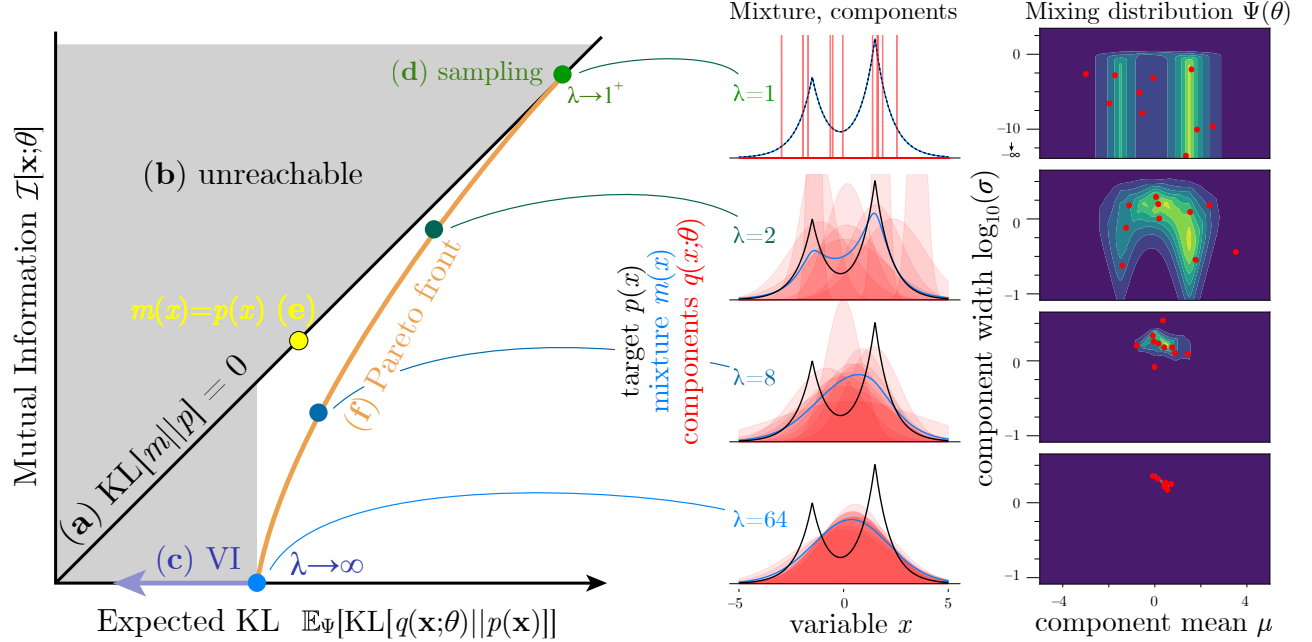


Figure 2: *Left*: Decomposition of $\text{KL}(m||p)$ into Mutual Information and Expected KL. **a**) Equation (4) implies that the asymptotic quality of any mixture (in terms of $\text{KL}(m||p)$) is given by its distance from the $y=x$ line (black diagonal line). **b**) Two unreachable regions are shaded in gray. The first is the region above the $y=x$ line, unreachable because $\text{KL}(m||p) \geq 0$. The second is the region to the left of the single-component variational solution, since VI achieves the minimum KL for any one component q . **c**) When $m(\mathbf{x}) = q(\mathbf{x}; \theta^*)$ as in classic VI, Expected KL is at its minimum and Mutual Information is zero. In our framework, this is achieved in the $\lambda \rightarrow \infty$ limit. Increasing the expressivity of q corresponds to moving left along the x-axis (blue arrow). **d**) Because sampling is asymptotically unbiased, it is a mixture that lives on the $\text{KL}(m||p) = 0$ or $y = x$ line. If \mathbf{x} is discrete, the coordinates of the point marked (d) are $(\mathcal{H}[\mathbf{x}], \mathcal{H}[\mathbf{x}])$, i.e. the entropy of $p(\mathbf{x})$. When \mathbf{x} is continuous, both Mutual Information and Expected KL grow unboundedly together as the individual mixture components approach Dirac deltas. In our framework, the $m(\mathbf{x})$ mixture behaves like classic sampling as $\lambda \rightarrow 1^+$. **e**) Any point on the $y=x$ line implies $m(\mathbf{x}) = p(\mathbf{x})$, and this may be possible to achieve without resorting to Dirac-delta mixture components (sampling) for certain combinations of p and q . However, points such as (e) are not guaranteed to exist for all problems, and are difficult to find due to the intractability of Mutual Information. **f**) By maximizing (an approximate version of) equation (5) with respect to $\psi(\theta)$ for different values of λ , a curve is traced out that connects VI to sampling in a natural and principled way. This curve depends on the specific form of the components $q(\mathbf{x}; \theta)$. *Middle*: Examples in a 1D toy problem, where $p(\mathbf{x})$ is an unequal mixture of two heavy-tailed distributions (black lines), and $q(\mathbf{x}; \theta)$ is a single Gaussian component with parameters $\theta = \{\mu, \log \sigma\}$ (translucent red components). *Right*: Varying λ controls the mixing distribution over θ (contours). Red sampled points on the right correspond to the components on the left.

that each achieve a different balance between Expected KL and Mutual Information (Figure 2f). Remarkably, this optimization problem leads naturally to a family of infinite stochastic mixtures with sampling and VI as special cases, as formalized by the following theorem:

Theorem 1 *Maximizing (5) with respect to ψ with $\lambda \rightarrow 1^+$ results in sampling-like mixtures where $m(\mathbf{x}) = p(\mathbf{x})$ and individual mixture components shrink to Dirac-deltas. When $\lambda \rightarrow \infty$, the mixture behaves like classic VI, with $\psi(\theta) \rightarrow \delta(\theta - \theta^*)$, and $m(\mathbf{x}) = q(\mathbf{x}; \theta^*)$. Proof: see Appendix A.1.*

Note that a condition for sampling-like behavior at $\lambda \rightarrow 1^+$ is that the component family q must be unimodal and capable of expressing Dirac-deltas, such as if q is a location-scale family. A condition for VI-like behavior is that θ^* is unique. Importantly, these are conditions only on the *interpretation* of (5) as generalizing sampling and VI; there are no such restrictions on *using* our framework with other component families. Other component families, such as multi-modal q , may in fact perform better in terms of the bias/variance trade-off discussed in the next section.

Theorem 1 establishes a framework for constructing

mixtures that behave like VI at one extreme (Figure 2c) and like sampling at the other (Figure 2d), by varying a single hyperparameter, $\lambda \in [1, \infty)$. A simple demonstration is shown in the right half of Figure 2, where a bimodal and heavy-tailed $p(\mathbf{x})$ is approximated by a mixture of Gaussians. Notice that the hypothetical infinite mixture, $m(\mathbf{x})$ (blue line, middle column) is unbiased for $\lambda = 1$ and approaches the single-component VI solution as λ grows. This demonstration was created using the method outlined in Section 4 (numerical details in Appendix B.3).

3.3 Navigating Bias/Variance Trade-Offs

While Theorem 1 characterizes solutions to the optimization problem in (5) at extremal values of λ , we now address intermediate values of λ and how they “interpolate” sampling and VI in terms of bias and variance. In general, bias and variance of approximate inference depend on the particular downstream application. A common problem is to approximate the expected value of some function f of interest, $\mathbb{E}_p[f(\mathbf{x})]$, by substituting the approximate distribution $\mathbb{E}_{m_T}[f(\mathbf{x})]$. In Figure 3, we compute the bias and variance on a randomly chosen degree-4 polynomial for each of three toy distributions with $T = 10$ (further details in Appendix B.4). Despite the arbitrarily-chosen f , a clear trend emerges where intermediate values of λ *smoothly interpolate* between sampling and VI in terms of both bias and variance.

To formalize this bias/variance trade-off in terms that are independent of f , we decompose the expected error of a T -component mixture into two terms:

$$\text{Total Error} = \mathbb{E}[\text{KL}(m_T(\mathbf{x})||p(\mathbf{x}))] = \underbrace{\text{KL}(m(\mathbf{x})||p(\mathbf{x}))}_{\text{bias}} + \underbrace{\mathbb{E}[\text{KL}(m_T(\mathbf{x})||m(\mathbf{x}))]}_{\text{variance}}. \quad (6)$$

Further, the variance term is related to Mutual Information between \mathbf{x} and θ :

$$\text{variance} \approx \frac{1}{T} \mathcal{I}[\mathbf{x}; \theta] \quad (7)$$

(see Appendix A.2). This is analogous to the variance of a Monte Carlo estimator of $\mathbb{E}[f]$ using T independent samples, which is $\frac{1}{T} \text{var}(f)$. Intuitively, $\mathcal{I}[\mathbf{x}; \theta]$ quantifies variance because it can be interpreted as the logarithm of the number of *distinguishable components* in the mixture, and a greater number of components implies that the variance of $\mathbb{E}_{m_T}[f(\mathbf{x})]$ may be larger. Thus, the following theorem establishes monotonic changes in bias and variance with λ in terms that are effectively independent of f :

Theorem 2 *Maximizing (5) with respect to ψ gives rise to a family of mixtures, parameterized by $\lambda \in$*

$[1, \infty)$. As λ increases, $\text{KL}(m||p)$ (bias) increases and $\mathcal{I}[\mathbf{x}; \theta]$ (approximate variance) decreases continuously and monotonically. Proof: see Appendix A.3.

4 MCMC SAMPLING OF COMPONENT PARAMETERS

4.1 A Tractable Mutual Information Approximation

Maximizing Mutual Information, as is required by (5), is a notoriously difficult problem that arises in many domains, and there is a large collection of approximations and bounds in the literature (Jaakkola and Jordan, 1998; Brunel and Nadal, 1998; Gershman et al., 2012; Wei and Stocker, 2016; Kolchinsky and Tracey, 2017; Poole et al., 2019). Here, we seek an approximation to Mutual Information that does not require knowing $m(\mathbf{x})$, that requires only local information about $\psi(\theta)$, and that can be evaluated separately for each θ . These properties will allow us to use MCMC methods to serially sample θ values from $\psi(\theta)$.

To derive such an approximation, note that Mutual Information between \mathbf{x} and θ can be written as

$$\mathcal{I}[\mathbf{x}; \theta] = \mathcal{H}[\theta] - \underbrace{\mathbb{E}_{\psi(\theta)}[\mathcal{H}[\hat{\theta}|\mathbf{x}]]}_{\mathcal{H}[\hat{\theta}|\theta]} \quad (8)$$

where $\mathcal{H}[\theta]$ is the entropy of $\psi(\theta)$ and $\mathcal{H}[\hat{\theta}|\mathbf{x}]$ is the entropy of $q(\hat{\theta}|\mathbf{x}) = \frac{q(\mathbf{x}; \hat{\theta})\psi(\hat{\theta})}{m(\mathbf{x})}$, i.e. the distribution of *inferred* θ values for a given \mathbf{x} . This second term, $\mathcal{H}[\hat{\theta}|\theta]$, can be thought of in terms of a statistical estimation problem, where each θ generates an \mathbf{x} , and $\hat{\theta}$ is the “recovered” value of θ . Bounding the error of $\hat{\theta}$ is a well-studied problem in statistics.

A lower-bound on Mutual Information can be derived from an *upper bound* on $\mathcal{H}[\hat{\theta}|\theta]$ for each θ – in other words, by upper-bounding the entropy of an estimator of the parameter θ . For this, we draw inspiration from Stam’s inequality (Stam, 1959; Dembo et al., 1991; Wei and Stocker, 2016), which states

$$\mathcal{H}[\hat{\theta}|\theta] \leq \frac{1}{2} \log |2\pi e \mathcal{F}(\theta)^{-1}|, \quad (9)$$

where $|\cdot|$ is a determinant, and $\mathcal{F}(\theta)$ is the Fisher Information Matrix, defined as

$$\mathcal{F}(\theta)_{ij} = -\mathbb{E}_{q(\mathbf{x}; \theta)} \left[\frac{\partial^2}{\partial \theta_i \partial \theta_j} \log q(\mathbf{x}; \theta) \right].$$

The Fisher Information Matrix is also the local metric on the *statistical manifold* with coordinates θ (Amari, 2016), it quantifies how “distinguishable” θ is from $\theta + d\theta$. Note that (9) can be viewed as the entropy

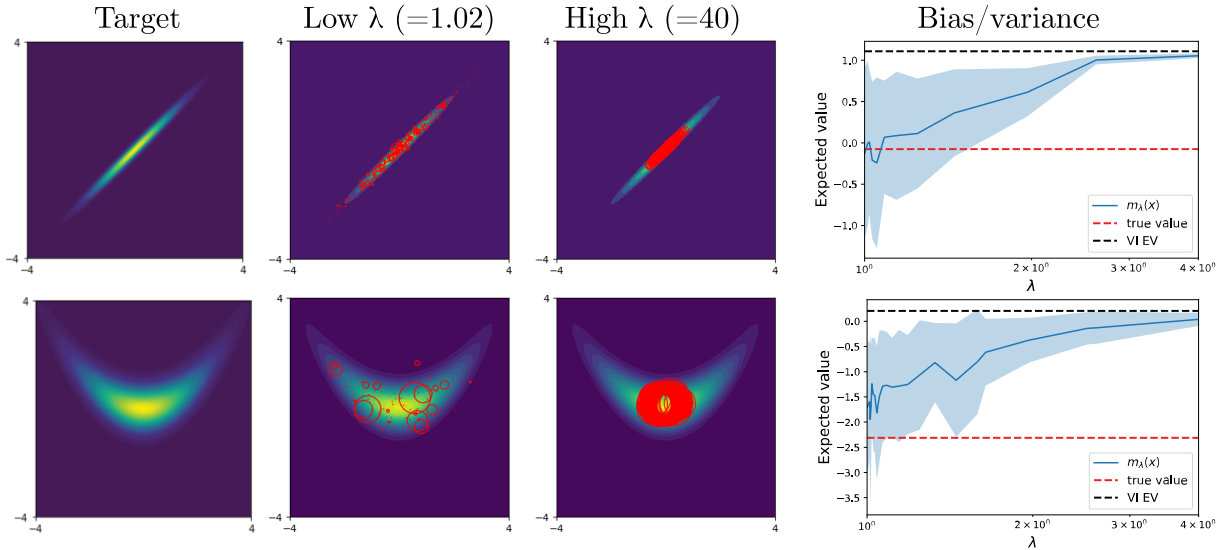


Figure 3: The parameter λ controls a bias/variance tradeoff. For two target distributions (left column), we sampled isotropic Gaussian distributions with an HMC chain at various values of λ (see Appendix B for sampling details). We then calculated the mean and variance of the expected value of a random 4th-order polynomial when using $T = 10$ samples (right column). Low λ provides unbiased but high variance estimators, while high λ provides a bias near that of standard VI and a vanishing variance.

of a Gaussian approximation to $q(\hat{\theta}|\mathbf{x})$ with precision matrix $\mathcal{F}(\theta)$; this Gaussian approximation is most accurate when $q(\mathbf{x}; \theta)$ itself is narrow and approximately Gaussian (Wei and Stocker, 2016).

Combining (8) and (9), we propose to use

$$\mathcal{I}_{\mathcal{F}}[\mathbf{x}; \theta] \equiv \mathcal{H}[\theta] - \frac{1}{2} \mathbb{E}_{\psi(\theta)} [\log |2\pi e \mathcal{F}(\theta)^{-1}|] \quad (10)$$

as a proxy for the intractable $\mathcal{I}[\mathbf{x}; \theta]$ in the optimization problem in (5).

Note that $\mathcal{I}_{\mathcal{F}}[\mathbf{x}; \theta]$ is not strictly a *bound* on $\mathcal{I}[\mathbf{x}; \theta]$, but may be seen as an *approximation* to it (Wei and Stocker, 2016). Briefly, this is because the original Stam’s inequality, as stated in (9), assumes θ is a scalar location parameter, and assumes the high-precision limit where $q(\hat{\theta}|\mathbf{x})$ is well-approximated by a Gaussian. Despite this, $\mathcal{I}_{\mathcal{F}}[\mathbf{x}; \theta]$ is well-suited for our purposes, since (i) it leads to remarkably simple expressions for $\psi(\theta)$ below; (ii) it is concave in ψ ; (iii) it is exact in the “sampling” limit using narrow Gaussian-like components (where $\mathcal{F}(\theta)$ is the precision matrix of $q(\hat{\theta}|\mathbf{x})$); (iv) in the large- λ limit Expected KL still dominates $\mathcal{I}_{\mathcal{F}}[\mathbf{x}; \theta]$, and (v) finally, the inequality in (9) is likely strict in cases where the entropy of $\psi(\theta)$ itself is small (i.e. large λ), since it neglects this additional prior information contained in $\psi(\theta)$ when estimating $\hat{\theta}$ and therefore over-estimates the entropy of

$q(\hat{\theta}|\mathbf{x})$.² Importantly, points (ii)–(iv) in this list are enough to ensure that Theorems 1 and 2 still hold, i.e. that substituting $\mathcal{I}_{\mathcal{F}}[\mathbf{x}; \theta]$ for $\mathcal{I}[\mathbf{x}; \theta]$ in our original optimization problem (5) results in families of mixture-approximations that effectively interpolate sampling and VI. However, (10) is most applicable when using Gaussian or Gaussian-like components, and that the monotonicity arguments in Theorem 2 now hold with respect to $\mathcal{I}_{\mathcal{F}}[\mathbf{x}; \theta]$ rather than $\mathcal{I}[\mathbf{x}; \theta]$.

4.2 Sampling Mixture Components

Combining (5) and (10) and applying the calculus of variations to optimize with respect to the mixing distribution ψ gives

$$\log \psi(\theta) = \frac{1}{2} \log |\mathcal{F}(\theta)| - \lambda \text{KL}(q(\mathbf{x}; \theta) \| p^*(\mathbf{x})) + C, \quad (11)$$

where C is constant with respect to θ (but depends on λ). Equation (11) is strikingly simple, and amenable to many existing MCMC sampling methods for drawing samples of θ from ψ . In particular, there are highly efficient samplers such as Hamiltonian Monte Carlo (HMC) (Neal, 2010) and variants such as the No-U-Turn Sampler (Hoffman and Gelman, 2014) which re-

²By analogy to the Bayesian Cramér-Rao bound (Gill and Levit, 1995; Fauß et al., 2021), a tighter variant of (9) might be applied here, though possibly at the expense of added complexity; we leave this to future work.

quire only gradients of the unnormalized log density,

$$\nabla_{\theta} \log \psi(\theta) = \frac{1}{2} \nabla_{\theta} \log |\mathcal{F}(\theta)| - \lambda \nabla_{\theta} \text{KL}(q||p). \quad (12)$$

Both of these terms are readily computed: $\nabla_{\theta} \log |\mathcal{F}(\theta)|$ is known in closed-form for certain families of q such as commonly-used Multivariate Gaussians or can be estimated numerically. $\nabla_{\theta} \text{KL}(q||p)$ (or $\nabla_{\theta} \text{KL}(q||p^*)$) is simply the gradient of the objective from classic VI for which numerous estimators exist (Hoffman et al., 2013; Kucukelbir et al., 2017) and that are implemented in a variety of statistics toolboxes such as Stan (Carpenter et al., 2017) or PyMC (Salvatier et al., 2016). Some common estimators of $\nabla_{\theta} \text{KL}(q||p)$ are stochastic, e.g. by using batches of data (Hoffman et al., 2013), in which case sampling parameters $\theta \sim \psi(\theta)$ can be done using stochastic gradient methods from the MCMC sampling literature (Ma et al., 2015).

Simulations throughout this paper were done using (11)–(12), using HMC for sampling (Neal, 2010), implemented in PyTorch, NumPy, and SciPy (Paszke et al., 2019; Harris et al., 2020; Virtanen et al., 2020) and plotted using Matplotlib (Hunter, 2007) (details in Appendix B). All code is available publicly online; the repository URL will be shared after the double-blind review process is complete.

5 Resource-Limitations (Finite T)

5.1 Optimal Compromise Between Sampling and VI

Large λ (VI-like) wastes redundant computation when T is large, and small λ (sampling-like) requires large T to overcome its variance. In other words, an appropriate compromise between sampling and VI depends on the computational budget, T , of how many components can be evaluated. These trade-offs for different values of T are shown empirically on toy problems in Figure 4.

One way to select the optimal λ given a budget of T mixture components is to choose the λ that minimizes the total expected error, i.e. the sum of bias and variance in equation (6). By combining (4) with (7), this is

$$\text{Total Error} \approx \mathbb{E}[\text{KL}(q||p)] + \mathcal{I}[\mathbf{x}; \theta] \left(\frac{1}{T} - 1 \right).$$

Along the Pareto front (Figure 2f), λ defines the *slope*, or

$$\lambda = \frac{d\mathcal{I}[\mathbf{x}; \theta]/d\lambda}{d\mathbb{E}[\text{KL}(q||p)]/d\lambda}.$$

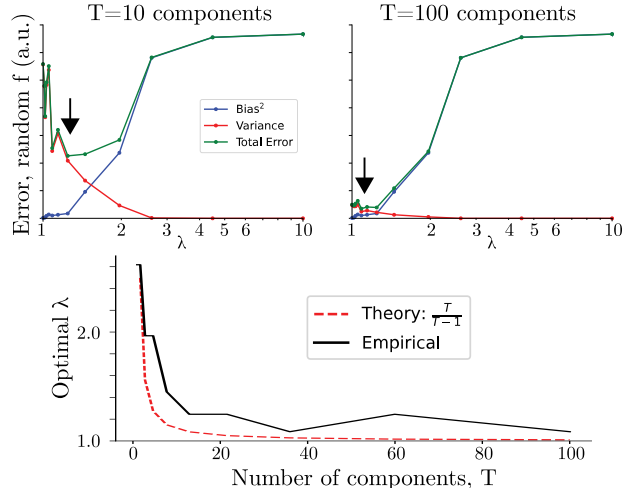


Figure 4: Minimizing Mean Squared Error for on a random polynomial selects $\lambda \approx 1.5$ for $T = 10$ samples (top left) and $\lambda \approx 1.1$ for $T = 100$ (top right). Bottom: The optimal λ closely follows the derived estimate in equation (13). Numerical results correspond to the first row of Figure 3 (see Appendix B.5).

Setting the derivative of Total Error to zero with respect to λ , we find that the optimal value is simply

$$\lambda^* = \frac{T}{T-1}. \quad (13)$$

Thus, when the computational budget is small (approaching $T = 1$ component), the optimal trade-off is to select $\lambda \rightarrow \infty$, i.e. VI-like behavior. Conversely, for large T , the optimal trade-off selects $\lambda \rightarrow 1^+$, i.e. sampling-like behavior. More generally, equation (13) is an easy recipe for navigating the trade-offs between sampling and VI given a fixed computational budget.

5.2 Time and Space Complexity

There are rapidly diminishing returns to increasing T , since Mutual Information is upper-bounded by $\mathcal{I}[\mathbf{x}; \theta] \leq \log T$, with equality only when all components are mutually non-overlapping (Jaakkola and Jordan, 1998). In past work using mixture approximations, these diminishing returns were compounded by $\mathcal{O}(T^2)$ time and $\mathcal{O}(T)$ space complexity, since solving the *joint* optimization problem over T components means selecting the parameters of each component depending on the other $T - 1$ components, all of which must be in memory at once (Jaakkola and Jordan, 1998; Gershman et al., 2012; Salimans et al., 2015; Miller et al., 2017; Acerbi, 2018) (but the $\mathcal{O}(T^2)$ complexity may be hardware-accelerated). We circumvent this by bounding Mutual Information using only *local* geometric information in (10), allowing each component to be selected independently of the others. This

means we can select and evaluate T components in $\mathcal{O}(T)$ time and either $\mathcal{O}(T)$ space (if all are stored) or $\mathcal{O}(1)$ space (if components are evaluated and accumulated online). Further, drawing samples of $\theta \sim \psi(\theta)$ is embarrassingly parallelizable into multiple sampling chains for a constant factor speedup.

6 DISCUSSION

Summary: Our work proposes a broad new family of approximate inference methods in which sampling methods are used in the space of variational parameters, resulting in stochastic mixture. Our main theoretical contribution is the framework shown in Figure 2, where an optimization problem that balances two objectives (Mutual Information and Expected KL) gives rise to a family of approximations that generalize and interpolate sampling and VI. We further derived an easy-to-use method to generate such mixtures using a convenient approximation to Mutual Information, which we then demonstrated and evaluated on toy problems.

Related Work: The trade-offs between sampling and VI are well-studied, and many methods have been proposed to “close the gap” between them (see (Angelino et al., 2016; Zhang et al., 2019) for general reviews). Like these other methods, we aim to provide good approximations with high computational efficiency and low variance.

There are many methods that use mixture models to reduce the bias of variational inference. In past work, mixtures are often directly optimized, reducing bias and maintaining low variance but at a $\mathcal{O}(T^2)$ computational cost using a mixture of T components (Section 5.2 above). Simplifications include using greedy optimization (Miller et al., 2017) or more efficient bounds on the Mutual Information term (Gershman et al., 2012). Our method reduces the cost per component at the expense of increased variance, since components may be independently sampled. Further, with some notable exceptions (Anaya-Izquierdo and Marriott, 2007; Salimans et al., 2015), most mixture VI methods make strong assumptions about the family of components (Jaakkola and Jordan, 1998; Gershman et al., 2012; Acerbi, 2018; Miller et al., 2017). While our general framework is agnostic to the family of q , our approximation in Section 4 is most applicable to Gaussian components.

Many methods use sampling in the service of variational inference, or vice versa, but do not provide a unifying approach to both. These typically use the samples to compute expectations used to update a variational approximation (Acerbi, 2018; Miller et al.,

2017; Kucukelbir et al., 2017), rather than to generate the mixture components themselves.

There are a large number of sampling approaches that aim to improve the efficiency of samples and reduce the variance of MCMC. Some of these use variational approaches as proposal distributions, but ultimately the posterior is approximated by a set of samples of the latent variables (de Freitas et al., 2001; Korattikara et al., 2014; Ma et al., 2015; Zhang et al., 2021). In contrast, by allowing samples over variational distributions, our approach allows each sample to cover more space with less variance and greater efficiency.

Despite some high-level similarities to other approaches, our framework is unusual in approximating the posterior by a sampled mixture of variational approximations. The Mixture Kalman filter (Chen and Liu, 2000) is a special case of this, which uses a sampled mixture of Gaussians, each constructed as a Kalman filter. A related approach is to *optimize* a parameterized function that generates mixture components (Salimans et al., 2015; Wolf et al., 2016), and generative diffusion models can also be seen as a case of this approach (Sohl-Dickstein et al., 2015; Ho et al., 2020). Our work differs in that we derived a closed-form mixing distribution that requires no additional learning or optimization.

Limitations and future work: On the theoretical side, there is a gap in generality going from $\mathcal{I}[\mathbf{x}; \theta]$ to $\mathcal{I}_{\mathcal{F}}$, since the latter is most appropriate for narrow and Gaussian-like components (Wei and Stocker, 2016). Incorporating prior information from $\psi(\theta)$ into this bound, generalizing to other kinds of components, or even starting with alternative bounds on $\mathcal{I}[\mathbf{x}; \theta]$ are all interesting avenues for future work. Another limitation is that in Section 5, we assumed that complexity is only a function of T not of λ ; in reality, λ changes the shape of ψ and can make it easier or harder to sample from efficiently.

Our biggest limitation in terms of implementation is scale, as we have only evaluated relatively simple toy distributions with a custom non-optimized implementation of HMC. A thorough comparison of our proposed family of methods with existing inference methods on larger problems will be an important next step. One interesting avenue to scale up our framework will be to combine insights from stochastic-gradient VI methods (Hoffman et al., 2013), with MCMC methods that make use of stochastic gradients of $\log p$ (Korattikara et al., 2014; Ma et al., 2015), i.e. making use of stochastic values of $\nabla \text{KL}(q||p)$ in (12).

References

- Luigi Acerbi. Variational Bayesian Monte Carlo. *Advances in Neural Information Processing Systems*, 2018.
- S Amari. *Information Geometry and Its Applications*. Applied Mathematical Sciences. Springer Japan, 2016.
- Karim Anaya-Izquierdo and Paul Marriott. Local mixture models of exponential families. *Bernoulli*, 13(3):623–640, 2007.
- Elaine Angelino, Matthew James Johnson, and Ryan P. Adams. Patterns of Scalable Bayesian Inference. *Foundations and Trends in Machine Learning*, 9(2-3):119–247, 2016.
- Christopher M Bishop. Pattern Recognition and Machine Learning. *Pattern Recognition*, page 738, 2006.
- Nicolas Brunel and Jean Pierre Nadal. Mutual Information, Fisher Information, and Population Coding. *Neural Computation*, 10(7):1731–1757, 1998.
- Bob Carpenter, Andrew Gelman, Matthew D. Hoffman, Daniel Lee, Ben Goodrich, Michael Betancourt, Marcus A. Brubaker, Jiqiang Guo, Peter Li, and Allen Riddell. Stan: A probabilistic programming language. *Journal of Statistical Software*, 76(1), 2017.
- Rong Chen and Jun S Liu. Mixture kalman filters. *Journal of the Royal Statistical Society: Series B (Statistical Methodology)*, 62(3):493–508, 2000.
- Nando de Freitas, Pedro Højten-Sørensen, Michael I. Jordan, and Stuart Russel. Variational MCMC. *Uncertainty in Artificial Intelligence*, 2001.
- Amir Dembo, Thomas M. Cover, and Joy A. Thomas. Information Theoretic Inequalities. *IEEE Transactions on Information Theory*, 37(6):1501–1518, 1991.
- Michael Fauß, Alex Dytso, and H. Vincent Poor. A variational interpretation of the Cramér–Rao bound. *Signal Processing*, 182, 2021.
- Samuel J. Gershman, Matthew D. Hoffman, and David M. Blei. Nonparametric Variational Inference. *Proceedings of the 29th International Conference on Machine Learning*, pages 235–242, 2012.
- Richard D. Gill and Boris Y. Levit. Applications of the van Trees inequality: A Bayesian Cramér–Rao bound. *Bernoulli*, 1(1):59–79, 1995.
- Charles R. Harris, K. Jarrod Millman, Stéfan J. van der Walt, Ralf Gommers, Pauli Virtanen, David Cournapeau, Eric Wieser, Julian Taylor, Sebastian Berg, Nathaniel J. Smith, Robert Kern, Matti Picus, Stephan Hoyer, Marten H. van Kerkwijk, Matthew Brett, Allan Haldane, Jaime Fernández del Río, Mark Wiebe, Pearu Peterson, Pierre Gérard-Marchant, Kevin Sheppard, Tyler Reddy, Warren Weckesser, Hameer Abbasi, Christoph Gohlke, and Travis E. Oliphant. Array programming with NumPy. *Nature*, 585(7825):357–362, September 2020.
- Jonathan Ho, Ajay Jain, and Pieter Abbeel. Denoising diffusion probabilistic models. *arXiv preprint arXiv:2006.11239*, 2020.
- Matthew D Hoffman and Andrew Gelman. The No-U-Turn Sampler: Adaptively Setting Path Lengths in Hamiltonian Monte Carlo. *Journal of Machine Learning Research*, 15:1351–1381, 2014.
- Matthew D. Hoffman, David M. Blei, Chong Wang, and John Paisley. Stochastic variational inference. *Journal of Machine Learning Research*, 14:1303–1347, 2013.
- John D. Hunter. Matplotlib: A 2d graphics environment. *Computing in Science Engineering*, 9(3):90–95, 2007.
- Tommi S. Jaakkola and Michael I. Jordan. Improving the Mean Field Approximation via the Use of Mixture Distributions. In Michael I. Jordan, editor, *Learning in Graphical Models*. Kluwer Academic Publishers, 1998.
- Artemy Kolchinsky and Brendan D. Tracey. Estimating mixture entropy with pairwise distances. *Entropy*, 19(7):1–17, 2017.
- Anoop Korattikara, Yutian Chen, and Max Welling. Austerity in MCMC Land: Cutting the Metropolis-Hastings Budget. *International Conference on Machine Learning*, 32(1):181–189, 2014.
- Alp Kucukelbir, David M. Blei, Andrew Gelman, Ramesh Ranganath, and Dustin Tran. Automatic Differentiation Variational Inference. *Journal of Machine Learning Research*, 18:1–45, 2017.
- Yi-An Ma, Tianqi Chen, and Emily B. Fox. A Complete Recipe for Stochastic Gradient MCMC. *Advances in Neural Information Processing Systems*, pages 1–16, 2015.
- Andrew C. Miller, Nicholas J. Foti, and Ryan P. Adams. Variational Boosting: Iteratively Refining Posterior Approximations. *arXiv*, 2017.
- Kevin P. Murphy. *Machine Learning: A Probabilistic Perspective*. The MIT Press, Cambridge, MA, 2012.
- Radford M. Neal. MCMC using Hamiltonian dynamics. *Handbook of Markov Chain Monte Carlo*, 2010.
- Adam Paszke, Sam Gross, Francisco Massa, Adam Lerer, James Bradbury, Gregory Chanan, Trevor Killeen, Zeming Lin, Natalia Gimelshein, Luca Antiga, Alban Desmaison, Andreas Kopf, Edward

- Yang, Zachary DeVito, Martin Raison, Alykhan Tejani, Sasank Chilamkurthy, Benoit Steiner, Lu Fang, Junjie Bai, and Soumith Chintala. Pytorch: An imperative style, high-performance deep learning library. In *Advances in Neural Information Processing Systems 32*, pages 8024–8035. Curran Associates, Inc., 2019.
- Ben Poole, Sherjil Ozair, Aaron van den Oord, Alexander A. Alemi, and George Tucker. On variational bounds of mutual information. *arXiv*, 2019.
- Tim Salimans, Diederik P. Kingma, and Max Welling. Markov Chain Monte Carlo and Variational Inference: Bridging the Gap. *Proceedings of the 32nd International Conference on Machine Learning*, pages 1218–1226, 2015.
- John Salvatier, Thomas V. Wieki, and Christopher Fonnesbeck. Probabilistic programming in Python using PyMC3. *PeerJ Computer Science*, 2016.
- Jascha Sohl-Dickstein, Eric Weiss, Niru Maheswaranathan, and Surya Ganguli. Deep unsupervised learning using nonequilibrium thermodynamics. In *International Conference on Machine Learning*, pages 2256–2265. PMLR, 2015.
- A. J. Stam. Some inequalities satisfied by the quantities of information of Fisher and Shannon. *Information and Control*, 2(2):101–112, 1959.
- Ole Tange. Gnu parallel 20201222 ('vaccine'), December 2020. GNU Parallel is a general parallelizer to run multiple serial command line programs in parallel without changing them.
- Pauli Virtanen, Ralf Gommers, Travis E. Oliphant, Matt Haberland, Tyler Reddy, David Cournapeau, Evgeni Burovski, Pearu Peterson, Warren Weckesser, Jonathan Bright, Stéfan J. van der Walt, Matthew Brett, Joshua Wilson, K. Jarrod Millman, Nikolay Mayorov, Andrew R. J. Nelson, Eric Jones, Robert Kern, Eric Larson, C J Carey, İlhan Polat, Yu Feng, Eric W. Moore, Jake VanderPlas, Denis Laxalde, Josef Perktold, Robert Cimrman, Ian Henriksen, E. A. Quintero, Charles R. Harris, Anne M. Archibald, Antônio H. Ribeiro, Fabian Pedregosa, Paul van Mulbregt, and SciPy 1.0 Contributors. SciPy 1.0: Fundamental Algorithms for Scientific Computing in Python. *Nature Methods*, 17:261–272, 2020.
- Martin J. Wainwright and Michael I. Jordan. Graphical Models, Exponential Families, and Variational Inference. *Foundations and Trends® in Machine Learning*, 1(1–2):1–305, 2008.
- Xue-Xin Wei and Alan A. Stocker. Mutual Information, Fisher Information, and Efficient Coding. *Neural computation*, 28(2), 2016.
- Christopher Wolf, Maximilian Karl, and Patrick van der Smagt. Variational inference with hamiltonian monte carlo. *arXiv preprint arXiv:1609.08203*, 2016.
- Cheng Zhang, Judith Butepage, Hedvig Kjellstrom, and Stephan Mandt. Advances in Variational Inference. *IEEE Transactions on Pattern Analysis and Machine Intelligence*, 41(8):2008–2026, 2019.
- Lu Zhang, Bob Carpenter, Andrew Gelman, and Aki Vehtari. Pathfinder: Parallel quasi-Newton variational inference. *arXiv*, 2021.

A PROOFS AND DERIVATIONS

Throughout, we assume that θ forms a minimal statistical manifold (Amari, 2016), so that whenever $q(\mathbf{x}; \theta_i) = q(\mathbf{x}; \theta_j)$ for all \mathbf{x} , it must be that $\theta_i = \theta_j$. Additional assumptions are introduced as-needed.

A.1 Proof of Theorem 1

Theorem 1 refers to the following optimization objective:

$$\mathcal{L}(\psi, \lambda) = \mathcal{I}[\mathbf{x}; \theta] - \lambda \mathbb{E}_{\psi(\theta)} [\text{KL}(q(\mathbf{x}; \theta) || p^*(\mathbf{x}))], \quad ((5) \text{ restated})$$

where $\lambda \in [1, \infty)$ is a hyper-parameter, and ψ is a probability density on θ . The two claims of the theorem are,

1. When $\lambda \rightarrow \infty$, the resulting mixture $m(\mathbf{x})$ “behaves like” classic variational inference.
2. When $\lambda \rightarrow 1$, the resulting mixture $m(\mathbf{x})$ “behaves like” classic sampling.

Both of these claims will be addressed both in the case of (5), and in the case of using the **approximate objective** in which $\mathcal{I}[\mathbf{x}; \theta]$ is replaced with

$$\mathcal{I}_{\mathcal{F}}[\mathbf{x}; \theta] \equiv \mathcal{H}[\theta] - \frac{1}{2} \mathbb{E}_{\psi(\theta)} [\log |2\pi e \mathcal{F}(\theta)^{-1}|]. \quad ((10) \text{ restated})$$

A.1.1 Claim 1: VI Behavior as $\lambda \rightarrow \infty$

Let θ^* be the set of values (or single value) of θ that minimize(s) $\text{KL}(q(\mathbf{x}; \theta) || p(\mathbf{x}))$. The minimal achievable value of $\mathbb{E}_{\psi}[\text{KL}(q || p)]$ for any ψ is likewise $\text{KL}(q(\mathbf{x}; \theta) || p(\mathbf{x}))$, which is achieved when $\psi(\theta)$ concentrates all of its mass on (some mixture of) θ^* . Each $q(\mathbf{x}; \theta^*)$ is considered a solution to the “classic” VI objective.

An equivalent objective to (5) is to maximize

$$\tilde{\mathcal{L}}(\psi, \lambda) = \frac{1}{\lambda} \mathcal{I}[\mathbf{x}; \theta] - \mathbb{E}_{\psi(\theta)} [\text{KL}(q(\mathbf{x}; \theta) || p^*(\mathbf{x}))],$$

which helps clarify that as $\lambda \rightarrow \infty$, a well-defined solution still exists, given by a mixture of deltas on θ^* values as just described. Further, among all such mixtures-of-deltas, the one with the maximum Mutual Information will give equal weight to each $q(\mathbf{x}; \theta^*)$ component (if they are mutually non-overlapping). Thus, whenever there is more than one optimal θ^* , $\psi(\theta)$ will be a mixture of components, each of which is a classic-VI solution. Such a mixture can only make $m(\mathbf{x})$ *less* biased than any one component is, since any $\psi(\theta)$ that is a weighted combination of deltas on θ^* points will have the same (minimal) Expected KL, and so increasing Mutual Information can only reduce $\text{KL}(m || p)$. When, instead, there is a single optimal θ^* values, $\psi(\theta)$ will concentrate to a single delta on that value as $\lambda \rightarrow \infty$.

If there are multiple optimal values of θ^* , and these values are *disconnected* in θ -space, then a sequential procedure for sampling $\theta \sim \psi(\theta)$ is unlikely to find more than a single one of these highly-peaked $\psi(\theta)$ modes. Thus, we can conclude that *in practice*, as $\lambda \rightarrow \infty$, $m(\mathbf{x})$ will behave like classic VI with a single component; and further, if multiple classic-VI modes are discovered, then this will perform *no worse* than the single-component solution (since increasing Mutual Information for a fixed Expected-KL can only reduce the total bias or $\text{KL}(m || p)$).

Approximate objective: Importantly, the core of this argument – that globally minimizing Expected KL selects the classic VI solution or a mixture of them – remains when maximizing $\mathcal{I}_{\mathcal{F}}[\mathbf{x}; \theta]$ rather than $\mathcal{I}[\mathbf{x}; \theta]$, hence VI remains a special case of our approximate framework introduced in Section 4 of the main paper. ■

A.1.2 Claim 2: Sampling Behavior as $\lambda \rightarrow 1$

Let us begin by defining what it means for $m(\mathbf{x})$ to be equivalent to sampling from $p(\mathbf{x})$. By this we mean that (i) all but negligibly many components shrink to Dirac-deltas, and (ii) these delta-components are selected at

each location \mathbf{x} with probability $p(\mathbf{x})$. When all components are deltas, expectations of any function, become equivalent to evaluating the function at those points and averaging:

$$\begin{aligned}\mathbb{E}_{m_T}[f(\mathbf{x})] &= \int_{\mathbf{x}} \left(\frac{1}{T} \sum_{t=1}^T \delta(\mathbf{x} - \mu(\theta^{(t)})) \right) f(\mathbf{x}) d\mathbf{x} \\ &= \frac{1}{T} \sum_{t=1}^T f(\mu(\theta^{(t)})),\end{aligned}$$

where $\mu(\theta)$ is a function that selects the mean of $q(\mathbf{x}; \theta)$.

Optimizing (5) with $\lambda = 1$ reduces to the original problem of selecting ψ to minimize $\text{KL}(m||p)$. As long as the $q(\mathbf{x}; \theta)$ component family can express Dirac-deltas at arbitrary μ s, this guarantees at least one such unbiased ψ , namely the one equivalent to sampling. However, it may be the case that there are *multiple* such unbiased mixing distributions, e.g. if $p(\mathbf{x})$ itself is a mixture of components from the q -family; in the two-dimensional space of Mutual Information versus Expected KL, such a mixture would appear as a point on the $y = x$ line (Figure 2e). Maximizing the objective in (5) does not arbitrate among these different unbiased ψ s if there is more than one. However, the *volume* of θ -space is larger in regions with large Fisher Information where mixture components are maximally distinguishable (Amari, 2016), i.e. where θ corresponds to deltas. Thus, we can conclude that if a process selects θ *uniformly* from among all unbiased ψ s, it is probable that $q(\mathbf{x}; \theta)$ will be very sharp in the sense of high Fisher Information.

This phenomenon can be seen in the $\lambda = 1$ panel on the right of Figure 2: some nonzero but negligible mass is placed on parts of θ -space where there are wide components. However, a much greater share of the mass in ψ is placed on narrow components. Because there is little difference at the scale of $p(\mathbf{x})$ between components with a width of 0.001 and components with a width of 0.0001, and so the marginal slices of $\psi(\theta)$ at these values are given essentially the same mass, resulting in the pattern of vertical stripes seen in the figure. Sampling from $\psi(\theta)$ almost always selects narrow components, since these constitute the bulk of the mass in θ -space (extending to infinitesimally narrow components, but the figure is truncated and the distribution normalized). The fraction of mass in $\psi(\theta)$ on non-delta components is vanishingly small, and so $m(\mathbf{x})$ behaves “almost always” like classic sampling with delta-like components.

Approximate objective: Two changes to this argument are worth noting when using the approximate objective introduced in Section 4, with $\mathcal{I}_{\mathcal{F}}[\mathbf{x}; \theta]$ instead of $\mathcal{I}[\mathbf{x}; \theta]$. First, $\mathcal{I}_{\mathcal{F}}[\mathbf{x}; \theta]$ is *strictly* concave in ψ , which follows from the strict concavity of $\mathcal{H}[\theta]$, whereas $\mathcal{I}[\mathbf{x}; \theta]$ is only concave (but not strictly so). The *strict* concavity of $\mathcal{I}_{\mathcal{F}}[\mathbf{x}; \theta]$ implies that a *unique* ψ will be selected for every λ . ■

Second, the bound is tight, i.e.

$$\mathcal{I}_{\mathcal{F}}[\mathbf{x}; \theta] \rightarrow \mathcal{I}[\mathbf{x}; \theta]$$

when

$$\mathcal{H}[\hat{\theta}|\theta] \rightarrow \frac{1}{2} \log |2\pi e \mathcal{F}(\theta)^{-1}|$$

(from the definitions of (9) and (10)). Consider using the following local Laplace approximation to $q(\hat{\theta}|\mathbf{x})$:

$$q(\hat{\theta}|\mathbf{x}) \approx \mathcal{N}(\hat{\theta}; \hat{\mu}, \hat{\Sigma}), \tag{A.1}$$

with

$$\begin{aligned}\hat{\mu} &= \mathbf{x} && \text{and} \\ \hat{\Sigma}^{-1} &= -\nabla_{\theta}^2 \log q(\mathbf{x}; \theta) \psi(\theta) \\ &= -\nabla_{\theta}^2 \log \psi(\theta) - \nabla_{\theta}^2 \log q(\mathbf{x}; \theta)\end{aligned}$$

where the Hessian ∇_{θ}^2 is evaluated at the value of θ with $\mu(\theta) = \mathbf{x}$. Combined with (8), the average entropy of this Laplace approximation gives an estimate of the entropy of $\mathcal{H}[\hat{\theta}|\theta]$:

$$\mathcal{H}[\hat{\theta}|\theta] \approx \mathbb{E}_{q(\mathbf{x}; \theta)} \left[\frac{1}{2} \log |2\pi e \hat{\Sigma}| \right].$$

In cases where the curvature of $\log q$ dominates the curvature of $\log \psi$ (i.e. $\nabla_{\theta}^2 \log q(\mathbf{x}; \theta) \gg \nabla_{\theta}^2 \log \psi(\theta)$), $\hat{\Sigma}$ in the Laplace approximation becomes

$$\hat{\Sigma} \rightarrow (-\nabla_{\theta}^2 \log q(\mathbf{x}; \theta))^{-1}.$$

Further, where $\log q(\mathbf{x}; \theta)$ has roughly constant curvature in expectation under \mathbf{x} , or when θ are the *natural parameters* of q ,

$$\nabla_{\theta}^2 \log q(\mathbf{x}; \theta) \rightarrow -\mathcal{F}(\theta).$$

Both of these conditions are met when $q(\mathbf{x}; \theta)$ shrinks towards a Dirac-delta. Taken together, this implies that $\mathcal{I}_{\mathcal{F}}[\mathbf{x}; \theta]$ approaches $\mathcal{I}[\mathbf{x}; \theta]$ in the limit where mixture components behave like samples. Thus, maximizing the *approximate* objective, $\mathcal{I}_{\mathcal{F}}[\mathbf{x}; \theta] - \lambda \mathbb{E}[\text{KL}(q||p)]$, as $\lambda \rightarrow 1$, selects the *unique* ψ that is both unbiased (because the bound can be made tight) and that consists of Dirac-delta components (because this is required in order for the bound to be tight). ■

A.2 Bias/Variance Trade-Off

A.2.1 Deriving Bias and Variance

When using T mixture components, as in

$$m_T(\mathbf{x}) = \frac{1}{T} \sum_{t=1}^T q(\mathbf{x}; \theta^{(t)}), \quad ((1) \text{ restated})$$

with $\theta^{(t)} \sim \psi(\theta)$, we would like to know the expected error to the true probability $p(\mathbf{x})$, or

$$\text{Total Error} = \mathbb{E}[\text{KL}(m_T(\mathbf{x})||p(\mathbf{x}))] \quad (\text{A.2})$$

where the outer expectation is taken over different draws of the T components. The Total Error can be decomposed into “bias” and “variance” terms as follows:

$$\mathbb{E}[\text{KL}(m_T(\mathbf{x})||p(\mathbf{x}))] = \underbrace{\text{KL}(m(\mathbf{x})||p(\mathbf{x}))}_{\text{bias}} + \underbrace{\mathbb{E}[\text{KL}(m_T(\mathbf{x})||m(\mathbf{x}))]}_{\text{variance}}, \quad ((6) \text{ restated})$$

which follows from the fact that $\mathbb{E}[m_T(\mathbf{x})] = m(\mathbf{x})$, which allows us to replace the outer expectation in the bias term with just $m(\mathbf{x})$.

The “bias” term is simply the objective we began with in equation (3) in the main text, which was then decomposed into Expected KL and Mutual Information in equation (4).

A.2.2 Upper-Bounding Variance

Next, we will show that the “variance” term with T components, $\text{var}(T) \equiv \mathbb{E}[\text{KL}(m_T(\mathbf{x})||m(\mathbf{x}))]$, is upper-bounded by

$$\text{var}(T) \leq \mathbb{E}_{\theta} \left[\int_{\mathbf{x}} q(\mathbf{x}; \theta) \log \frac{\alpha(T)q(\mathbf{x}; \theta) + (1 - \alpha(T))m(\mathbf{x})}{m(\mathbf{x})} d\mathbf{x} \right], \quad (\text{A.3})$$

where $\alpha(T) \equiv \frac{1}{T}$ is a weight that interpolates between $q(\mathbf{x}; \theta)$ and $m(\mathbf{x})$ in the numerator of the log. Note that the expectation inside $\text{var}(T)$ is over all $\{\theta^{(1)} \dots \theta^{(T)}\}$, and the expectation on the right is over a single θ . At $T = 1$, this tight because $\text{var}(1) = \mathbb{E}[\text{KL}(q||m)] = \mathcal{I}[\mathbf{x}; \theta]$, and as $T \rightarrow \infty$, this is tight because $\text{var}(T) \rightarrow 0$ and this bound goes to $\mathbb{E}[\text{KL}(m||m)]$, which is 0.

Proof: We begin by expanding out the definition of $\text{var}(T)$ as

$$\text{var}(T) = \mathbb{E} \left[\int_{\mathbf{x}} \left(\frac{1}{T} \sum_{t=1}^T q(\mathbf{x}; \theta^{(t)}) \right) \log \frac{m_T(\mathbf{x})}{m(\mathbf{x})} d\mathbf{x} \right].$$

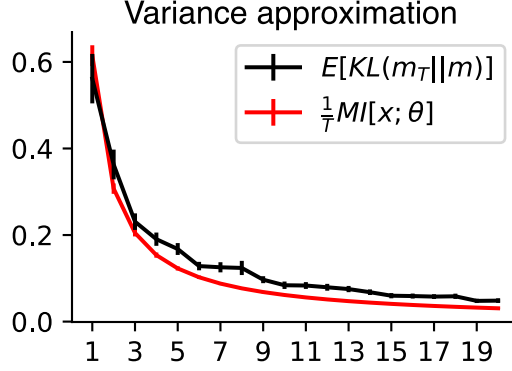


Figure A.1: Numerical check of the approximation to variance in equation (7) as a function of the number of components, T . The true variance is shown in black, and the approximation in (7) is shown in red. All values are computed using Monte Carlo estimators, and error bars indicate \pm Monte Carlo Standard Error (MCSE).

Next, we will pull the sum outside of the expectation, and break the expectation into t and $-t$ (not t) terms:

$$\text{var}(T) = \frac{1}{T} \sum_{t=1}^T \mathbb{E}_t \left[\mathbb{E}_{-t} \left[\int_{\mathbf{x}} q(\mathbf{x}; \theta^{(t)}) \log \frac{m_T(\mathbf{x})}{m(\mathbf{x})} d\mathbf{x} \right] \right].$$

Next, we will likewise break $m_T(\mathbf{x})$ into t and $-t$ terms, and push the expectation over $-t$ inwards:

$$\text{var}(T) = \frac{1}{T} \sum_{t=1}^T \mathbb{E}_t \left[\int_{\mathbf{x}} q(\mathbf{x}; \theta^{(t)}) \mathbb{E}_{-t} \left[\log \frac{\frac{1}{T} q(\mathbf{x}; \theta^{(t)}) + \frac{1}{T} \sum_{t' \neq t} q(\mathbf{x}; \theta^{(t')})}{m(\mathbf{x})} \right] d\mathbf{x} \right].$$

Applying Jensen's inequality to the expectation over $-t$ ($\mathbb{E}[\log f] \leq \log \mathbb{E}[f]$) gives the following bound:

$$\text{var}(T) \leq \frac{1}{T} \sum_{t=1}^T \mathbb{E}_t \left[\int_{\mathbf{x}} q(\mathbf{x}; \theta^{(t)}) \log \frac{\frac{1}{T} q(\mathbf{x}; \theta^{(t)}) + \mathbb{E}_{-t} \left[\frac{1}{T} \sum_{t' \neq t} q(\mathbf{x}; \theta^{(t')}) \right]}{m(\mathbf{x})} d\mathbf{x} \right].$$

Note that $\mathbb{E}_{-t} \left[\frac{1}{T} \sum_{t' \neq t} q(\mathbf{x}; \theta^{(t')}) \right] = \frac{T-1}{T} m(\mathbf{x})$, and so

$$\text{var}(T) \leq \frac{1}{T} \sum_{t=1}^T \mathbb{E}_t \left[\int_{\mathbf{x}} q(\mathbf{x}; \theta^{(t)}) \log \frac{\frac{1}{T} q(\mathbf{x}; \theta^{(t)}) + \frac{T-1}{T} m(\mathbf{x})}{m(\mathbf{x})} d\mathbf{x} \right].$$

Now that all references to t' and $-t$ have been dropped, the outer sum over $\sum_{t=1}^T$ can be dropped, as it is T copies of the same sum. Finally, since $\frac{T-1}{T} = 1 - \frac{1}{T}$, we arrive at

$$\text{var}(T) \leq \mathbb{E}_\theta \left[\int_{\mathbf{x}} q(\mathbf{x}; \theta) \log \frac{\alpha(T) q(\mathbf{x}; \theta) + (1 - \alpha(T)) m(\mathbf{x})}{m(\mathbf{x})} d\mathbf{x} \right],$$

with $\alpha(T) \equiv \frac{1}{T}$. ■

A.2.3 Approximating Variance

Applying Jensen's inequality to the numerator of the log gives a *lower bound* on this *upper bound*, which we denote by \leq :

$$\begin{aligned} \text{var}(T) &\leq \mathbb{E}_\theta \left[\int_{\mathbf{x}} q(\mathbf{x}; \theta) \left(\alpha(T) \log \frac{q(\mathbf{x}; \theta)}{m(\mathbf{x})} + (1 - \alpha(T)) \log \frac{m(\mathbf{x})}{m(\mathbf{x})} \right) d\mathbf{x} \right] \\ &= \mathbb{E}_\theta [\alpha(T) \text{KL}(q(\mathbf{x}; \theta) || m(\mathbf{x})) + (1 - \alpha(T)) \text{KL}(m(\mathbf{x}) || m(\mathbf{x}))], \end{aligned}$$

which then simplifies to

$$\text{var}(T) \leq \alpha(T) \mathbb{E}_\theta \left[\int_{\mathbf{x}} q(\mathbf{x}; \theta) \log \frac{q(\mathbf{x}; \theta)}{m(\mathbf{x})} \right] = \frac{1}{T} \mathcal{I}[\mathbf{x}; \theta],$$

which is the estimate used in the main paper in equation (7). This approximation is plotted in Figure A.1 for one example run of HMC, as described in Appendix B below.

A.3 Proof of Theorem 2

Theorem 2 claims that solutions to (5) for intermediate values of λ – along the Pareto front in Figure 2f – result in continuous and monotonic changes to both the “bias” or $\text{KL}(q||p)$ as well as the “variance” or $\mathcal{I}[\mathbf{x}; \theta]$ using the approximation from the previous section.

Both claims follow from the concavity properties of the objective with respect to changes in the ψ density. Mutual Information is well-known to be a concave functional (but not strictly) of each of its marginal distributions. For a fixed q family, let $\mathcal{I}[\psi]$ denote the Mutual Information between \mathbf{x} and θ using ψ as the mixing distribution. The concavity of \mathcal{I} means that

$$\mathcal{I}[\alpha\psi_1 + (1 - \alpha)\psi_2] \leq \alpha\mathcal{I}[\psi_1] + (1 - \alpha)\mathcal{I}[\psi_2],$$

for $0 \leq \alpha \leq 1$. The Expected KL term, or $\mathbb{E}_\psi[\text{KL}(q||p)]$, is *linear* with respect to changes in ψ . Further, both Mutual Information and Expected KL change smoothly with small changes in ψ .

Together, the concavity of Mutual Information and linearity of Expected KL imply that the total weighted objective in (5) is concave and smooth with respect to ψ for the relevant regime of $\lambda \in [1, \infty)$.

We would like to know the relative changes in the Pareto-optimal values of Mutual Information and Expected KL as λ changes, or

$$\frac{\partial}{\partial \lambda} \mathcal{I}[\mathbf{x}; \theta]^* \\ \frac{\partial}{\partial \lambda} \mathbb{E}[\text{KL}(q||p)]^*$$

using $*$ to denote that these are changes in the optimum. The Implicit Function Theorem applies, and λ itself is equal to the slope of the Pareto-front, or

$$\lambda = \frac{\partial \mathcal{I}[\mathbf{x}; \theta]^* / \partial \lambda}{\partial \mathbb{E}[\text{KL}(q||p)]^* / \partial \lambda}.$$

Further, since both Mutual Information and Expected KL are positive, as long as $\lambda > 1$, this implies that increasing λ results in (i) positive changes in $\mathcal{I}[\mathbf{x}; \theta]$, and (ii) positive but *smaller* changes in $\mathbb{E}[\text{KL}[q||p]]$. Thus,

$$\frac{\partial}{\partial \lambda} \mathcal{I}[\mathbf{x}; \theta]^* > 0,$$

which completes the proof of the statement that (approximate) variance increases monotonically with λ . Also, (ii) implies that

$$\frac{\partial}{\partial \lambda} \text{KL}(m||p) = (\mathbb{E}[\text{KL}(q||p)]^* - \mathcal{I}[\mathbf{x}; \theta]^*) < 0,$$

which completes the proof of the statement that variance decreases monotonically with λ . ■

B NUMERICAL DETAILS

All code to generate the figures in this paper is available publicly online; the repository URL will be shared after the double-blind review process is complete. Python libraries used include NumPy, SciPy, PyTorch, and Matplotlib (Harris et al., 2020; Virtanen et al., 2020; Paszke et al., 2019; Hunter, 2007). Jobs running sampling chains across a grid of parameters were managed using GNU Parallel (Tange, 2020).

We used three toy distributions in our results:

- The “banana” distribution over \mathbb{R}^2 , defined as

$$\log p(x, y) = -(y - (x/2)^2)^2 - (x/2)^2.$$

- The “cigar” distribution over \mathbb{R}^2 , which is a normal distribution with a marginal variance of 1 on both x and y and a correlation of 0.99.
- The “Laplace mixture” distribution over \mathbb{R}^1 , defined as

$$p(x) \propto 0.4e^{-\frac{|x+1.5|}{0.75}} + 0.6e^{-\frac{|x-1.5|}{0.75}}.$$

B.1 Hamiltonian Monte Carlo (HMC)

We implemented HMC (Neal, 2010) using PyTorch (Paszke et al., 2019) for automatic differentiation. We implemented a custom warm-up or tuning phase, starting with 200 randomly chosen “seed” points drawn from a zero-mean isotropic normal distribution of whatever dimension the space was that was being sampled. These points were then advanced, by gradient ascent, up the log probability for 100 steps. The average negative curvature of the log probability across the resulting set of points was used to set the mass in each dimension, passing the curvature through a softplus function to handle cases where average curvature was convex.

Each of these 200 seed points was then run for a single run of leapfrog integration to adapt the integration step size towards a target acceptance rate of 0.8 at a total integration time of 2.0 (Hoffman and Gelman, 2014). This completed the “tuning” phase.

Samples were then generated, and initial burn-in samples discarded, using the standard HMC procedure (Neal, 2010).

B.2 Details for Figure 1

A grid of $\mathbf{x} = (x, y)$ values were created for the underlying contour plot, using the “banana” distribution defined above. The “sampling” panel was created by running the HMC sampler described above directly on \mathbf{x} . The “variational” panel was created by initializing a random 2D Multivariate Normal with isotropic covariance, then using Newton’s method to optimize its parameters, $\theta = \{\mu_x, \mu_y, \log \sigma\}$ to minimize $\text{KL}(q||p)$. The “Proposed compromise” panel was created by running the same HMC sampler described above, but now on θ instead of \mathbf{x} , using $\log \psi(\theta)$ as defined in (11), with $\lambda = 2$.

B.3 Details for Figure 2

The sketch on the left of Figure 2 was done by hand. The panels on the right half of Figure 2 were generated using the “Laplace mixture” distribution described above. For each value of λ , we manually annotated a “window” of $\theta = \{\mu, \log \sigma\}$ values to plot. For each one, a grid of θ values was created and $\log \psi(\theta)$, using (11), was evaluated at every point in the grid. This was then transformed to a normalized distribution for the contour plots in the rightmost column of the figure. The mixtures were created by simply evaluating the weighted sum,

$$m(\mathbf{x}) = \sum_{\theta} \psi(\theta)q(\mathbf{x}; \theta)$$

for every θ in the grid. The red points and corresponding components were sampled directly from the discretized grid of $\psi(\theta)$ values using multinomial sampling.

B.4 Details for Figure 3

For each of the “banana” and “cigar” distributions, we ran a HMC sampler over θ as described in section B.2 above. We selected a grid of λ values and ran HMC for 10000 samples per value of λ .

To compute bias and variance, we generated a random polynomial of degree 4, where each coefficient of degree p was drawn from $\mathcal{N}(0, 1)/p!$. We estimated the unbiased expectation using scipy’s built-in quadrature integration tool `dblquad`. For each value of λ , we estimated bias using the full $m_{10000}(\mathbf{x})$ mixture. We then estimated the variance of $m_T(\mathbf{x})$ by subsampling T components from the full set of 10000 samples repeatedly and computing the sample variance of $\mathbb{E}_{m_T}[f]$. The integral of the random polynomial under each individual Gaussian kernel was computed using Gaussian quadrature using the Numpy function `hermgauss`.

B.5 Details for Figure 4

This figure uses the same 10,000 samples from the previously described HMC chains at each λ , as well as the variance of $\mathbb{E}_{m_T(\mathbf{x})}[f(\mathbf{x})] = \frac{1}{T} \sum_t \int_{\mathbf{x}} q(\mathbf{x}|\theta_t) f(\mathbf{x})$ as a function of T . Bias ($\text{KL}(m(\mathbf{x})\|p(\mathbf{x}))$) and variance ($\text{KL}(m_T(\mathbf{x})\|m(\mathbf{x}))$) were calculated as above for each T and λ . Then, for each T , we selected the minimum value of the mean-squared error of the expected function as the selected value.